Glycoconjugate Journal (1998) **15:** 187–191

EGC2
Studies on the conformational behaviour of GlcNAc-Man_3-$GlcNAc_2$ oligosaccharides using molecular dynamics simulations

Tibor Kozar*, Igor Tvaroska† and Jeremy P. Carver‡

GlycoDesign Inc., 480 University Avenue, Suite 900, Toronto, Ontario, Canada M5G 1V2

Three-dimensional structures of the natural substrate unit for the enzyme *N*-acetylglucosamine-transferase II, GlcNAc-Man_3-$GlcNAc_2$, were investigated by molecular modelling methods. Molecular dynamics (MD) and molecular mechanics calculations on two hexasaccharides, namely GlcNAc-Man_3-$GlcNAc_2$-Asn and GlcNAc-Man_3-$GlcNAc_2$-OMe were performed by the Biosym/MSI software using the CVFF and CFF95 force fields in vacuum. The MD simulations were calculated for 3 ns at different simulation temperatures and for two values of dielectric constant, $\epsilon = 1$ and $\epsilon = 4$. From each 3 ns trajectory, 3050 structures have been optimized. The local minima obtained have been clustered into families exhibiting similar values of glycosidic torsional angles ϕ, ψ, and ω. The influence of the simulation conditions and force fields used on the conformational behaviour and structure of the title oligosaccharides is discussed.

Keywords: **hexasaccharides, molecular modelling, three-dimensional structure**

Introduction

Knowledge of the three-dimensional structure and dynamic behaviour of the natural substrates for the enzymes involved in the biosynthetic pathway generating the glycan moieties of glycoproteins is important for understanding the molecular features required for the design of inhibitors for these enzymes. In this communication, we report the results obtained from the molecular modelling of GlcNAc-Man_3-$GlcNAc_2$-Asn and GlcNAc-Man_3-$GlcNAc_2$-OMe oligosaccharides. The GlcNAc-Man_3-$GlcNAc_2$ unit is the substrate for elongation by several glycosyl transferases. The *N*-acetylglucosamine-transferase II substitutes at a distinct position on the tri-mannosyl core of this unit to initiate 'branches' [1, 2]. An increased amount of the $(1 \rightarrow 6)$-linked GlcNAc residues (one of the branching positions) has been noted in primary tumours of various carcinoma and also appears to correlate with disease progression [3, 4]. The enzymes involved in the processing of GlcNAc branched structures are obvious targets for inhibitors. Therefore, the determination of the three-dimensional structures and conformational flexibility of natural substrates for the *N*-acetylglucosamine-transferases is of great interest.

Materials and methods

Oligosaccharides

Two hexasaccharides, namely

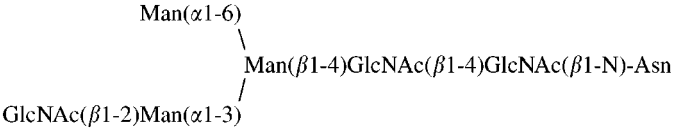

(1)

and

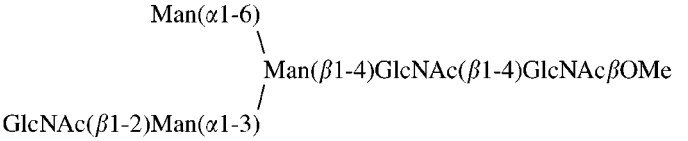

(2)

have been studied.

The Φ and Ψ glycosidic torsion angles are defined as H1-C1-O1-CX′ and C1-O1-CX′-HX′, where X is 2, 3, 4 according to the type of linkage $(1 \rightarrow 2, 1 \rightarrow 3, 1 \rightarrow 4)$. For the $1 \rightarrow 6$ linkage Φ, Ψ and ω are defined as H1-C1-O1-C6′, C1-O1-C6′-C5′ and O1-C6′-C5′-H5′, respectively.

* On leave from the Institute of Experimental Physics, Slovak Academy of Sciences, Kosice, and the †Institute of Chemistry, Slovak Academy of Sciences, Bratislava, Slovak Republic.
‡ To whom correspondence should be adressed. E-mail: *tibor@glycodesign.com; †igor@glycodesign.com; ‡jpcarver@glycodesign.com.

0282–0080

Molecular dynamic simulations and molecular mechanics calculations

The Biosym/MSI modelling software (InsightII/Discover [5, 6]) running on an SGI Power Indigo R8000 has been used to perform molecular dynamics and molecular mechanics calculations applying the CVFF and CFF95 [7] force fields. Molecular dynamics trajectories were calculated with 0.5 integration step, 250 fs saving interval, 50 ps equilibration and 3 ns data production. The simulation temperatures were 300 K and 400 K and different values of dielectric constant ($\varepsilon = 1$ and $\varepsilon = 4$) have been used for the electrostatic energy contribution. In the next step, all 3050 geometries from each of the simulations (1 ps snapshots) were optimized. An ensemble of optimized structures was further processed and non-identical conformations have been clustered into families with similar values of glycosidic torsional angles Φ, Ψ, and ω using in-house software.

Results and discussion

Flexibility around glycosidic linkages

An analysis of all molecular dynamics (MD) simulations revealed a considerable amount of flexibility exhibited by (1) and (2) within the conformational space of glycosidic torsional angles. This was observed independently of the simulation conditions, *ie*, force field, dielectric constant, and simulation temperature. For each glycosidic bond of (1) and (2), there are several conformational regions which resemble those usually found on the (Φ, Ψ) maps of corresponding disaccharides [8, 9]. On the other hand, it appeared that temperature and ε influence significantly the frequency of the transitions between different regions of conformational maps.

Examples of two-dimensional conformational maps are presented in Figure 1 for disaccharide subunits of (1). MD simulations with the CVFF force field (400 K and $\varepsilon = 4$) show that the dominant region for the GlcNAcβ(1-4) GlcNAc linkage is centred at $\Phi = 40^\circ$ and $\Psi = 0^\circ$ (Figure 1a). Conformational transitions of this linkage were identified also in regions centred around (20°, −40°), (130°, −40°), (160°, 0°), (40°, −160°), (0°, 180°), and (160°, −160°). The last three conformational regions were not populated on the corresponding map of (2). The most noticeable difference observed for simulations with $\varepsilon = 1$ is a significantly larger occupancy of the (160°, 0°) region for both molecules.

In MD simulations with the CFF95 force field (T = 300 K, $\varepsilon = 1$) contrary to the corresponding simulation with the CVFF, no transitions to the *trans* region

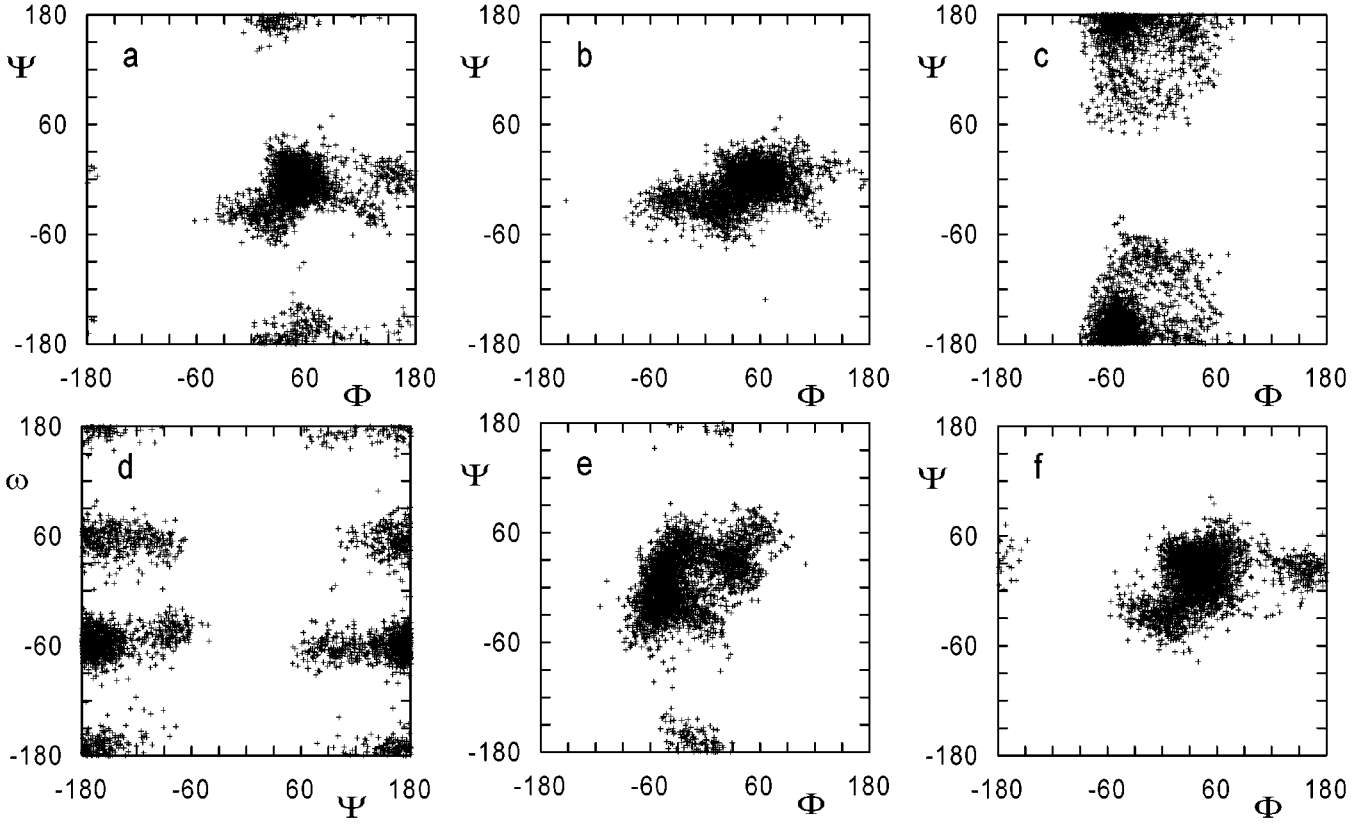

Figure 1. Two-dimensional plots of the distribution of Φ, Ψ and ω glycosidic torsion angles resulted from 3.05 ns molecular dynamics simulation (CVFF force field, 400 K, $\varepsilon = 4$) of (1). Assignment of the disaccharide subunits: (a) GlcNAc(β1-4)GlcNAc; (b) Man(β1-4)GlcNAc; (c) Man(α1-6)Man, (Φ, Ψ); (d) Man(α1-6)Man, (Ψ, ω); (e) Man(α1-3)Man; (f) GlcNAc(β1-2)Man.

(160°, 0°) were observed on the 3 ns time scale and the molecule fluctuated between other low energy regions. However, the simulation at 400 K and $\varepsilon = 4$ using CFF95 found frequent transitions between all low energy wells.

Four trajectories (at 400 K and $\varepsilon = 4$) for the second β-(1 → 4) glycosidic linkage (Manβ(1-4)GlcNAc) (Figure 1b) gave similar results for both force fields for both (1) and (2). Results of the simulations at 300 K, $\varepsilon = 1$ or $\varepsilon = 4$ are more divergent. For example, an irreversible transition to the region centered at (60°, −180°) occurred at an early stage of the CFF95 simulation of (1) (300 K, $\varepsilon = 1$). In contrast, the equivalent simulation of (2) (CFF95, 300 K, $\varepsilon = 1$) revealed transitions between three conformational regions (120, −30°), (160, 0°), and (−20°, 60°).

In accordance with the previous conformational studies on (1 → 6) linkages [9–12], no transitions away from the region at $\Phi \sim -60°$ were observed during the course of the 3 ns simulation for the Manα(1-6)Man linkage (Figure 1c), regardless of the simulation parameters. The trajectories for the second bond (Ψ) of this linkage showed frequent transitions between three major energy wells located at $\Psi \sim -170°$, −90° and +70°. For the C5–C6 bond (ω) conformational transitions occurred between all three possible staggered orientations (Figure 1d), usually designated *GT* ($\omega \sim -60°$), *GG* (180°), and *TG* (+60°).

The Manα(1-3)Man linkage showed frequent transitions between three major energy wells (Figure 1e) during simulations with both force fields and $\varepsilon = 4$, which correspond closely to the low energy regions identified for this disaccharide [9, 13]. These results resemble MD simulations of the corresponding disaccharide using the CHARM program [14]. However, a completely different picture was obtained from the simulation using the CVFF (300 K, $\varepsilon = 1$) force field. In this simulation, after approximately 100 ps, both molecules underwent a transition from the initial conformation to the region centred at (−20°, 180°). The molecules then fluctuated in this region during the remainder of the simulations.

The GlcNAc residue of the GlcNAcβ(1-2)Man linkage is a terminal sugar unit of the hexasaccharides. The main conformational region for this bond (Figure 1f) is around 30–50° for the Φ angle but an additional stable conformational domain around 160° resulted from several simulations. For the Ψ direction, fluctuations are observed in a low

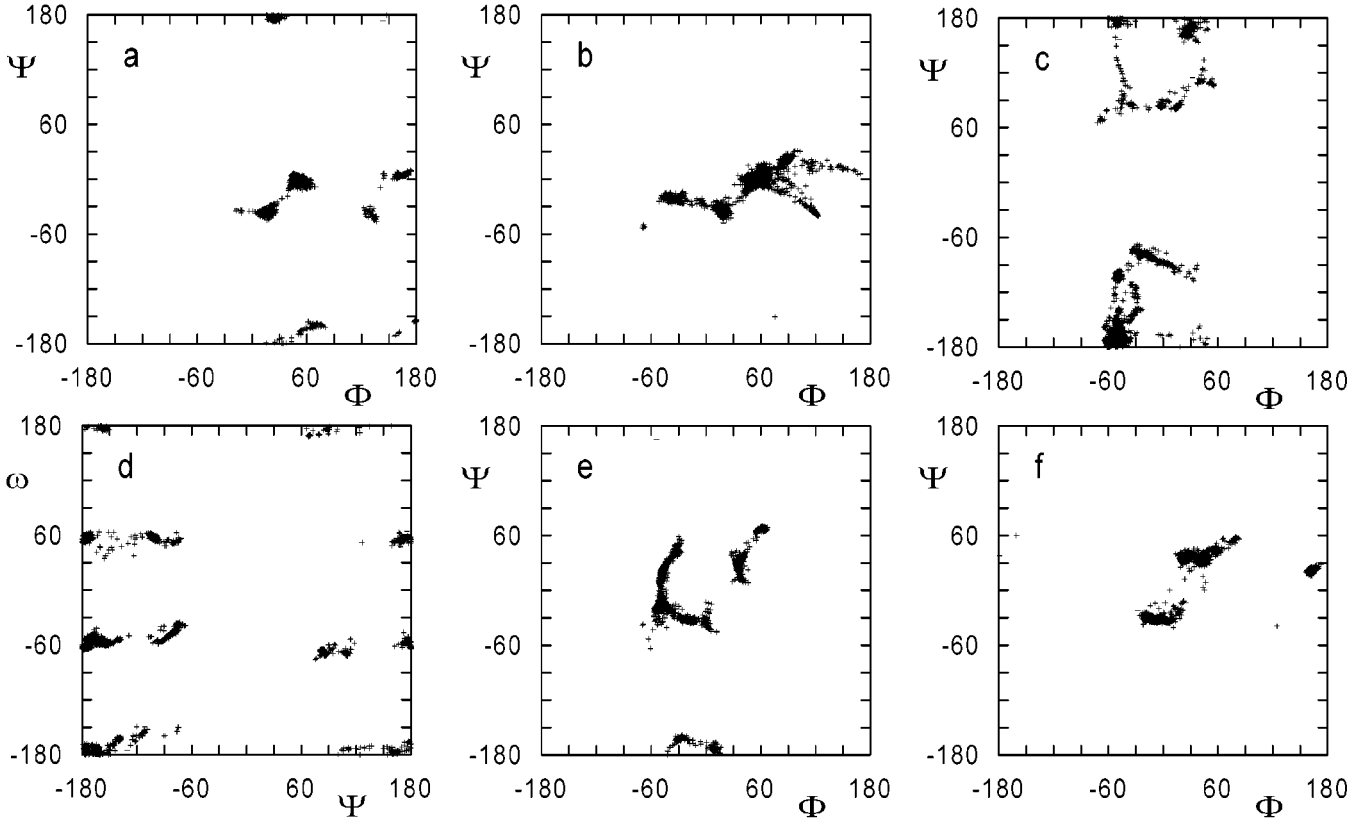

Figure 2. Two-dimensional plots of the optimized values of Φ, Ψ, and ω glycosidic torsion angles as resulted from the minimization of 3050 structures from 3.05 molecular dynamics trajectory of (1) presented in Figure 1. The assignment of the maps is the same as in Figure 1.

Table. 1 Comparison of the geometry optimization and clustering of local minima calculated by the CFF95 and CVFF for GlcNAc-Man_3-$GlcNAc_2$-Asn (1) and GlcNAc-Man_3-$GlcNAc_2$-OMe (2). The number of starting structures (n), number of optimized conformers (*m*), number of clusters (*p*), number of clusters contributing to the conformational equilibrium (*x*), and the number of conformers in the latter clusters (*w*) are listed.

	T [K]	*ε*	*n*	*m*	*p*	*x*	*w*
GlcNAc-Man_3-$GlcNAc_2$-Asn (1)							
CVFF	300	1	6615	632	37	12	526
CVFF	400	1	2048	862	102	18	564
CVFF	400	4	3051	3051	481	36	1584
CFF95	300	1	3051	1890	174	39	1037
CFF95	400	1	3051	1909	303	2	312
CFF95	300	4	3051	2988	213	53	2256
CFF95	400	4	3051	3007	456	42	1597
GlcNAc-Man_3-$GlcNAc_2$-OMe (2)							
CVFF	300	1	6596	471	65	12	170
CVFF	400	1	4341	1524	182	17	316
CVFF	400	4	3051	3051	391	62	2259
CFF95	300	1	3051	856	100	3	228
CFF95	400	1	3051	1435	201	6	552
CFF95	300	4	3051	3007	121	26	2568
CFF95	400	4	1551	1535	357	75	938

Table 2. Comparison of the mean values of glycosidic torsional angles *Φ*, *Ψ*, *ω* for the most favored cluster of GlcNAc-Man_3-$GlcNAc_2$-Asn (1) and GlcNAc-Man_3-$GlcNAc_2$-OMe (2) and time-averaged values from 3 ns simulations (*italic*) using the CFF95 and CVFF force fields. Number of conformers in the cluster (*n*) and relative population of the cluster (*x*) are also listed. Reference data [15, 16] on similar molecules are also included.

	T [K]	*ε*	*n*	*Glycosidic torsional angles*											
				GlcNAc → GlcNAc		*Man → GlcNAc*		*Man → Man*			*Man → Man*		*GlcNAc → Man*		
				Φ1	*Ψ1*	*Φ2*	*Ψ2*	*Φ3*	*Ψ3*	*ω3*	*Φ4*	*Ψ4*	*Φ5*	*Φ5*	*x [%]*
GlcNAc-Man_3-$GlcNAc_2$-Asn (1)															
CFF95	300	1	21	49	– 4	49	– 170	– 50	178	– 45	31	45	169	20	67
CFF95	300	4	86	41	– 19	95	– 167	– 53	120	171	8	– 61	60	51	36
CFF95	400	1	300	173	1	170	2	– 24	– 141	– 174	– 8	– 171	52	53	100
CFF95	400	4	203	60	– 7	74	34	– 51	– 164	– 51	– 33	52	17	50	35
CFF95	*400*	*4*	*3050*	*38*	*– 27*	*50*	*– 7*	*– 42*	*– 174*	*– 73*	*– 25*	*– 11*	*41*	*49*	
CVFF	300	1	96	158	2	162	7	– 33	73	163	– 15	– 166	49	35	85
CVFF	400	1	41	162	5	59	– 10	– 35	– 76	– 33	34	30	140	26	74
CVFF	400	4	281	47	0	59	1	– 54	– 174	– 58	– 46	22	27	36	67
CVFF	*400*	*4*	*3050*	*50*	*– 8*	*44*	*– 8*	*– 35*	*174*	*– 50*	*– 22*	*10*	*40*	*17*	
Lommerse *et al.* [16],			conf A	52	7	47	– 10	– 1	180	– 123					
			conf B	62	10	47	– 9	– 14	– 177	– 54					
			conf C	49	8	38	– 13	– 1	– 179	– 114					
Shaanan *et al.* [15]				47	10	43	– 38	– 63	76	– 66	– 34	7			
GlcNAc-Man_3-$GlcNAc_2$-OMe (2)															
CFF95	300	1	194	55	– 20	166	2	18	– 165	180	5	– 175	– 175	35	94
CFF95	300	4	441	64	– 15	74	36	– 51	– 165	– 51	– 33	52	18	50	47
CFF95	400	1	369	171	0	171	0	– 22	– 141	– 174	– 4	– 171	45	49	100
CFF95	400	4	39	22	– 48	109	– 30	– 14	– 129	– 179	9	– 59	57	53	30
CFF95	*400*	*4*	*3050*	*38*	*– 25*	*45*	*– 19*	*– 30*	*– 178*	*174*	*– 23*	*– 27*	*45*	*48*	
CVFF	300	1	42	156	1	156	8	– 35	– 137	– 161	– 15	– 168	60	40	99
CVFF	400	1	4	161	3	161	7	– 34	– 157	– 173	– 21	– 162	25	– 13	83
CVFF	400	4	435	49	– 1	61	3	– 53	– 173	– 58	– 46	22	28	37	55
CVFF	*400*	*4*	*3050*	*51*	*– 8*	*48*	*– 7*	*– 33*	*– 171*	*– 59*	*– 28*	*8*	*37*	*14*	

energy region between $-60°$ and $90°$ with transitions between minima located at $\sim 30°$ and $-20°$.

Three-dimensional shape (conformation)

Figure 2 shows the populations of all local minima that resulted from the optimization of 3050 structures generated for (1) during the 3 ns MD simulations. As would be expected, the (Φ, Ψ) maps for the individual linkages within the minimized structures are clustered in minima that occupy less space than in the corresponding plots from the entire MD simulations (Figure 1). On the other hand, the differences in the spread of these clusters on the (Φ, Ψ) maps indicates considerable differences in the flexibility of individual glycosidic linkages of (1).

Table 1 summarizes the results of the optimization and clustering and demonstrates how a change in ε influences the resulting flexibility of hexasaccharide in the simulation. When $\varepsilon = 1$ was used in the calculations, the conformational equilibrium was usually dominated by a single, highly populated cluster. Conformations in such clusters are stabilized by an intramolecular network of hydrogen bonding. In contrast, the calculations with $\varepsilon = 4$ gave a more complex conformational equilibrium with the population of the most favoured cluster at less than 50%.

The average values of the glycosidic torsion angles for the most favoured cluster of (1) and (2) are listed in Table 2 together with the mean values (in italic) obtained from the 3 ns MD simulations. The corresponding data from experimental studies on related oligosaccharides are also included. Unfortunately, experimental structural data for (1) or (2) are not available. The reference molecules are slightly different, including additional sugar units (*eg* fucose linked to protein-bound GlcNAc), which might have an impact on overall molecular flexibility. Therefore, the comparison is only qualitative. Nevertheless, independent of the different monosaccharide composition and molecular environment, the conformational preference for the GlcNAc-GlcNAc-Man fragment and in part, also the α(1-6) bonded mannose, as obtained from simulation at 400 K and $\varepsilon = 4$, matches the molecular shape, as inferred from experimental data, well [15–17].

Acknowledgements

The short-term grace licence of the CFF95 force field from Molecular Simulations Inc. is gratefully acknowledged.

References

1 Schachter H (1986) *Biochem Cell Biol* **64**: 163–81.
2 Kornfeld R, Kornfeld S (1985) *Ann Rev Biochem* **54**: 631–64.
3 Hakomori S-I (1989) *Adv Cancer Res* **52**: 257–31.
4 Dennis JW (1991) In *Cell Surface Carbohydrates and Cell Development* (Fukuda M, ed.) pp 161–94. Boca Raton: CRC Press.
5 *InsightII User Guide*, October 1995. San Diego: Biosym/MSI, 1995.
6 *Discover User Guide*, October 1995. San Diego: Biosym/MSI, 1995.
7 *CFF95 User Guide*, October 1995. San Diego: Biosym/MSI, 1995.
8 Imberty A, Delage MM, Bourne Y, Cambillau C, Pérez S (1991) *Glycoconjugate J* **8**: 456–83.
9 Imberty A, Pérez S, Hricovíni M, Shah RN, Carver JP (1993) *Int J Biol Macromol* **17**: 17–23.
10 Tvaroska I, Pérez S, Marchessault R (1978) *Carbohyd Res* **61**: 97–106.
11 Brisson J-R, Carver JP (1983) *Biochemistry* **22**: 1362–68.
12 Qasba PK, Balaji PV, Rao VSR (1994) *Glycobiology* **4**: 805–15.
13 Rutherford TJ, Partridge J, Weller CT, Homans SW (1993) *Biochemistry* **32**: 12715–24.
14 Carver JP, Mandel D, Michnick SW, Imberty A, Brady JW (1990) In *Computer Modeling of Carbohydrate Molecules* ACS Symposium Series Vol. 430 (French AD, Brady JW, eds) pp 266–80. Washington DC: American Chemical Society.
15 Shaanan B, Lis H, Sharon N (1991) *Science* **254**: 862.
16 Lommerse JPM, Kroon-Batenburg LMJ, Kroon J, Kamerling JP, Vliegenhart JFG (1995) *J Biomolecular NMR* **5**: 79–94.
17 Lommerse JPM, Kroon-Batenburg LMJ, Kamerling JP, Vliegenhart JFG (1995) *Biochemistry* **34**: 8196–206.